

The long term polarimetric variability of the strongly magnetic white dwarf Grw+70° 8247

S. Bagnulo¹ and J.D. Landstreet^{1,2}

¹*Armagh Observatory and Planetarium, College Hill, Armagh BT61 9DG, UK. E-mail: Stefano.Bagnulo@Armagh.ac.uk; John.Landstreet@Armagh.ac.uk*

²*Department of Physics & Astronomy, University of Western Ontario, London, Ontario, Canada N6A 3K7 E-mail: jlandstr@uwo.ca*

Accepted 2019 April 11. Received 2019 April 10; in original form 2019 February 17

ABSTRACT

Some of the white dwarfs exhibit among the strongest magnetic fields in the universe. Many of these degenerate magnetic stars are also rotating very slowly. Among these objects, Grw+70° 8247, with its century-long suspected rotation period and its 400 MG magnetic field, stands as a particularly interesting object. Surprisingly, for this star, the first white dwarf in which a magnetic field was discovered, no spectropolarimetric observations have been discussed in the literature in the last 40 years. Here we present two sets of linear and circular polarisation spectra taken in 2015 and 2018, and we compare them with spectropolarimetric data obtained in the 1970s. Polarisation shows variability over a time interval of four decades, but some subtle changes may have been detected even over a three year time interval. Using the variation of the polarisation position angle as a proxy for the rotation of the magnetic axis in the plane of the sky, we conclude that the star's rotation period probably lies in the range of 10^2 to 10^3 years. Our data analysis is accompanied by a description of our various calibrations and tests of the ISIS instrument at the William Herschel Telescope that may be of general interest for linear spectropolarimetric measurements. We also found discrepancies in the sign of circular polarisation as reported in the literature, and made explicit the definitions that we have adopted.

Key words: polarization – stars: white dwarfs – stars: magnetic fields – stars: individuals: Grw+70° 8247

1 INTRODUCTION

A small percentage of white dwarfs (WDs) exhibit a magnetic field organised on a large scale over the stellar surface, probably the fossil remnant of a field that originated during an earlier stage of the star's life. The mean magnitude of such fields ranges over more than five dex of strength, from a few kG to about 1000 MG, and can have important physical effects on the host star, for example by transferring angular momentum internally and exchanging it with circumstellar material, and through suppressing atmospheric and envelope convection under many circumstances.

In a larger context, the fields of the magnetic white dwarfs (MWDs) are an example of the occasional occurrence of large static fields in a variety of stars during stellar evolution, including upper main sequence stars, white dwarfs, and neutron stars. The origin of these fields is still essentially completely mysterious. This phenomenon may be capable of providing valuable information on specific evolutionary paths (for example, of merging binary systems) that at present cannot be exploited because we have not understood some basic stellar processes. In addition, the fields of white

dwarfs provide access to a plasma laboratory permeated by fields far too large to be generated statically in terrestrial laboratories.

Up to a field strength of the order of 80 or 100 MG, white dwarf fields are detected and studied using the splitting, shifting and polarisation of spectral lines. For higher field strengths, spectral lines are smeared almost out of recognition but the fields may be identified through the broad-band continuum circular and linear polarisation usually observed throughout the optical and ultraviolet wavelength windows (Ferrario et al. 2015), as well as through (usually very shallow) broad spectral features in the flux spectra.

Beyond identifying magnetic fields in white dwarfs, and estimating the magnitude of the magnetic field, it is of considerable interest to try to understand the distribution of field strength and direction over the stellar surface. This kind of information can help to clarify the interaction of the field with other physical processes in the underlying star, and may provide clues about the still unclear processes that lead to the occurrence of magnetic fields in a small fraction of white dwarfs.

Study of field structure generally requires observing the star repeatedly as it rotates. A number of magnetic white dwarfs exhibit short term variability, with a period that is associated to the star's rotation period (typically from a few hours to a few days). As in the case of the better studied magnetic chemically peculiar stars of the main sequence (Ap stars), the magnetic variability is explained in terms of a magnetic field not symmetric about the rotation axis, so that the observer sees a magnetic configuration that changes as the star rotates. This oblique rotator model was proposed to explain the polarimetric behaviour of the magnetic Ap stars by [Stibbs \(1950\)](#), and since then has been the basic model adopted for any large-scale stellar field that is not currently sustained by dynamo action.

Only about two dozen of the several hundred known MWDs have been clearly identified as having very high magnetic fields, above about 100 MG (e.g. [Ferrario et al. 2015](#), Fig. 5). About half of these 100+ MG stars have emerged from the very large lists of new white dwarfs found as by-products of the Sloan Digital Sky Survey (SDSS). The other very high field MWDs were mostly found before the first data release from the SDSS by a variety of means, including surveys of broad-band circular polarisation or discovery of remarkable flux spectra (flux spectra are usually denoted here as Stokes I spectra).

For the SDSS very high field MWDs, in general a single low S/N (typically in the range of 10 to 30), low resolution ($R \sim 2000$) spectrum is available, and the characteristic field strength assigned is usually found by comparing the observed spectrum to spectra from a large grid of pre-computed flux spectra of MWDs of a large range of T_{eff} and field strength. The field structure assumed for the grid is a combination of low order multipoles, often dominated by a dipole. The WD atmosphere is assumed to be pure H, and only the spectrum of H is included in the model spectra, with spectral line positions taken from tables of atomic level splitting in very large fields such as those of [Wunner et al. \(1985\)](#). The computation of the grid spectra and comparison with observed I spectra is described in detail by [Jordan \(1992\)](#); [Euchner et al. \(2002\)](#) and [Külebi et al. \(2009\)](#).

This method of modelling provides a first, basic characterisation of typical field strength and a possible, but not unique, and almost certainly highly simplified, magnetic field geometry. It takes no account of the possibility that the field may look rather different as seen from different sides of the MWD as it rotates, and makes no use of information that may be contained in the linear and/or circular polarisation spectra (Stokes components Q , U , and V). The results of such an analysis provide information about the general magnitude of the field and possibly of the spread of field strength over the hemisphere visible at the time that the spectrum was taken, but little further information.

For most of the dozen or so earlier discovered, and generally brighter, very high field MWDs, more information is often available. For example, several Stokes I spectra may have been taken, or spectra in non-optical wavelength regions such as the UV may be available, or there may be polarisation spectra (often of circularly polarised light, Stokes V , sometimes of the linear polarisation components Q and U). For four of the 100+ MG field MWDs the rotation period is known, so data taken during a reasonably short interval could be assigned to distinct lines of sight to the MWD.

When rotational phase-resolved data are available, models of the surface magnetic field strength and structure may be considerably better constrained. An excellent example of the quality of modelling that can be achieved when several phase-resolved spectra of both Stokes I and V are available is the analysis of PG 1015+014 carried out by [Euchner et al. \(2006\)](#) on the basis of modelling tools developed by [Jordan \(1992\)](#) and [Euchner et al. \(2002\)](#). Their results clearly show that the field of this star is dominated by regions with local field strength mostly in the range of 70–80 MG, and provide fairly well constrained low resolution maps of the large-scale distribution of flux over the surface.

However, although models have been developed for each of the four highest-field MWDs with known rotation periods, none of these four MWDs have been observed systematically enough to make it possible to try to model a series of phase-resolved flux and polarisation spectra.

Remarkably, for several of the earliest discovered and most intensely studied high-field magnetic white dwarfs, including the prototype, Grw+70° 8247 = WD 1900+705¹, it is not even clear whether any real variations have been detected. Since any magnetic configuration not strictly symmetric about the rotation axis of the star should lead to some kind of observable variability as the underlying star rotates, these non-varying stars are suspected of having extremely long rotation periods, of the order of decades or centuries (as is also the case for a few middle main sequence magnetic Ap stars, e.g. [Mathys 2017](#)). For the MWDs in the tranche with fields above 100 MG, variability may have been detected, but no rotation periods have been established that are longer than 1.4 days.

For these high-field stars, searching for modest levels of variability of polarisation through broad-band filters over time spans of decades is not straightforward. Both filter bandpasses and detector wavelength sensitivity change with time and technology, and observed variations may simply be the caused by a different sampling of the stellar polarised spectrum. The information content of filter polarimetry is also quite limited.

There is little doubt that the most robust method of identifying variability, measuring the rotation period, and obtaining spectral information useful for modelling and mapping the field structure, is to repeatedly obtain polarised spectra through large wavelength windows (say 2000 Å or more), using high enough spectral resolution so that measurements taken over time with different instruments can be reliably compared. Perhaps surprisingly, this has so far hardly been done, even though at least two current facility spectropolarimeters, ISIS at the William Herschel Telescope of the ING, and FORS at the ESO VLT, are quite capable of measuring both circular and linear continuum polarisation accurately over large wavelength ranges, and have been capable of doing this for at least two decades. Fortunately, for a few of the brightest, most strongly magnetic and highly polarised white dwarfs, some low resolution archival spec-

¹ In addition to being the first magnetic white dwarf discovered, and the first high-field MWD, Grw+70° 8247 (which was identified and catalogued in the Greenwich Observatory zone of the Astrogaphic Catalogue) was only the fifth white dwarf ever identified ([Kuiper 1935](#)).

tropolarimetry is available for comparison with modern data (Angel et al. 1972; Landstreet & Angel 1974, 1975; Angel et al. 1985; Schmidt et al. 1996).

In this paper we present new moderate resolution line and continuum spectropolarimetry for Grw+70° 8247, and we compare our data to archival spectropolarimetry. It has not yet been established that Grw+70° 8247 is actually variable, and on the basis of apparently constant data available decades ago it has been suggested that this white dwarf may be rotating with a period of order 10^2 yr or more.

The search for subtle variations in the stellar polarised spectra has prompted us to pay particular attention to the characterisation of the polarimetric module of the instrument(s) employed in our observations, so that if differences between new spectropolarimetry and archival data are found, we can be reasonably sure that they are not due to instrumental artefacts in the old or the new data.

2 DEFINITIONS OF THE OBSERVED POLARISATION, WITH A SPECIAL ATTENTION TO THE SIGN OF CIRCULAR POLARISATION

In this paper we will consider the reduced Stokes parameters $P_X = X/I$ (where $X = Q, U, V$) and the corresponding null profiles N_X . It will also be useful to describe the linear polarisation in terms of the fraction of linear polarisation $P_L = (P_Q^2 + P_U^2)^{1/2}$ and its position angle Θ , such that $P_Q = P_L \cos(2\Theta)$ and $P_U = P_L \sin(2\Theta)$. The Stokes parameters are defined according to Shurcliff (1962), and for linear polarisation we have adopted as a reference direction the great circle passing through the object and the North Celestial Pole. The position angle of the linear polarisation Θ is measured positive looking at the source, counting counter-clockwise from the great circle passing through the object and the North Celestial pole.

The two representations of linear polarisation (P_Q, P_U) and (P_L, Θ) are equivalent, but from the physical and geometrical point of view, (P_L, Θ) may be more convenient for a physical understanding of variability and discrepancies. In case of the observations of standard stars, an incorrect alignment of the polarimetric optics is promptly detected by a discrepancy in the position angle of the polarisation. The position angle of polarisation due to the presence of a magnetic field is directly influenced by the transverse components of the magnetic field; for instance, in the Zeeman regime, and neglecting the magneto-optical effects, the direction of the maximum polarisation is parallel to the projected magnetic axis (e.g. Landolfi et al. 1993). For small polarisation values, the position angle is not well defined, and may be dramatically affected even by small amounts of instrumental polarisation or other spurious effects; therefore sometimes the representation (P_Q, P_U) will be more convenient. In this paper, to report our observations of unpolarised standard stars, we will adopt the (P_Q, P_U) representation; to report our observations of standard stars for linear polarisation we will adopt the (P_L, Θ) representation. For our primary target, which is a magnetic star but has a polarisation close to zero at certain wavelength ranges, we will describe the linear polarisation both with (P_Q, P_U) and with (P_L, Θ).

Our main target, Grw+70° 8247, is usually thought of

as a star with circular polarisation approximately constant with time (and as such it was often suggested as a standard star for circular polarisation). However, it is found that literature data of circular polarisation measured in similar interval wavelength ranges have sometimes discrepant signs. For instance, Kemp et al. (1970b) and Angel & Landstreet (1970b) reported a positive sign; Landstreet & Angel (1975) and Butters et al. (2009) a negative value. This sign ambiguity is probably related to the adoption of different definitions of the Stokes parameters, and in particular of the sign of circular polarisation, as discussed for instance by Clarke (1974), Landi Degl’Innocenti et al. (2007) and Bagnulo et al. (2009).

In this work we adopt the definition given in Landi Degl’Innocenti & Landolfi (2004), Landi Degl’Innocenti et al. (2007) and Bagnulo et al. (2009), and consistent with Shurcliff (1962), i.e., circular polarisation is *positive* (or *right-handed*) when the tip of the electric field vector is seen to rotate *clockwise* in a fixed plane perpendicular to the propagation of the light, looking at the source. As explained in Bagnulo & Landstreet (2018), we determine the sign of our polarisation measurements by measuring the longitudinal field of well known magnetic stars using the weak-field relationship (e.g. Bagnulo et al. 2002)

$$\frac{V}{I} = -g_{\text{eff}} 4.67 \cdot 10^{-13} \lambda^2 \frac{1}{I} \frac{dI}{d\lambda} \langle B_z \rangle \quad (1)$$

which tells us that a positive longitudinal field will cause Stokes V to be positive in the blue wing of an absorption line and negative in the red wing. Some magnetic Ap stars that have been found with constant polarity over decades may be used as reference stars; for instance HD 94660 and γ Equ (since the 1970s) are always reported with a negative longitudinal field, and our field measurements of γ Equ are indeed consistent with a negative sign (see Sect. 5.4). Of course our empirical approach to link the sign of circular polarisation to the sign of the magnetic field just shifts the problem into the original determination of the polarity of the magnetic field of well known magnetic stars, which probably goes back to the extensive work on Ap stars by Babcock (1958).

The ambiguity in the sign of circular polarisation does not seem to have affected the sign of the magnetic field reported in the literature. For instance, we note that Putney (1995) reports a negative circular polarisation for Grw+70° 8247 (see her Fig. 1c), i.e., with the sign opposite to what we measure. However, for the field determinations of MWDs in the Zeeman regime, she adopts Eq. (1) with the plus sign in its right hand term, and so other authors do (e.g. Borra & Landstreet 1980). This suggests that the sign of stellar magnetic fields are probably defined consistently in most if not all literature.

Removing the ambiguity in the sign of circular polarisation is obviously crucial to allow one a proper comparison of the observations of different authors and epochs. Establishing the geometrical significance of the sign of the circular polarisation is also important when the original of circular polarisation is associated to homochirality.

3 NEW OBSERVATIONS: INSTRUMENT SETTINGS

We carried out our new spectropolarimetric observations with the ISIS instrument of the William Herschel Telescope. The ISIS polarimetric module consists of an achromatic retarder waveplate ($\lambda/2$ for observations of linear polarisation, or $\lambda/4$ for observations of circular polarisation) which can be rotated to a series of fixed positions, followed by a Savart plate that splits the incoming radiation into two beams linearly polarised in directions perpendicular to each other, one along the principal plane of the plate (the parallel beam f^{\parallel}), and one perpendicular to that plane (the perpendicular beam f^{\perp}). These beams propagate parallel to each other but separated. A special $18''$ dekker prevents the superposition of each beam split by the Savart plate with the light coming from the other parts of the observed field of view. The use of a dichroic beam splitter with cut-off centred at 5300 \AA allows us to observe simultaneously in the blue arm with grating R600B (which we have set at a central wavelength = 4400 \AA so as to cover the spectral range of $3700\text{--}5300 \text{ \AA}$), and in the red arm with grating R1200R (central wavelength = 6500 \AA , to cover the spectral range $6100\text{--}6900 \text{ \AA}$). Our observations were obtained with slit width of $1.0''$, $1.2''$ and $2.0''$ for a spectral resolving power R of 2500, 2050 and 1280 in the blue arm, and 8950, 7100 and 4500 in the red arm, respectively. Spectral features of Grw+70° 8247 are broad enough that observations obtained at the lowest resolution with the $2''$ slit width did not appear more smeared than those obtained at the highest resolution with a $1''$ slit width.

For Grw+70° 8247 we have obtained three observations of circular polarisation, two in August 2015 and one in November 2018, and two observations of linear polarisation, one in August 2015 and one in November 2018. During the November 2018 run (night 21 to 22), we obtained an additional set of observations both in circular and linear polarisation, but the selection of a wrong combination of dekker and window readout did not allow us to record the background. Therefore, both datasets obtained on the night of November 21 were discarded.

For our measurements we adopted the use of the beam swapping technique (e.g. Bagnulo et al. 2009) which minimises the impact of instrumental polarisation. ISIS circular polarisation measurements were obtained using a series of four exposures with the $\lambda/4$ retarder waveplate set at position angles -45° , $+45^\circ$, $+45^\circ$, -45° , while our linear polarisation measurements were obtained with a series of eight exposures with the $\lambda/2$ waveplate set at position angles 0° , 22.5° , 45° , 67.5° , 90° , 112.5° , 135° and 157.5° .

The redundancy of our observing strategy allows us to measure also the so called null profiles N_X , which give us an experimental estimate of the uncertainties (Donati et al. 1997; Bagnulo et al. 2009).

The dates and times of the new observations, along with other data to be explained later, are listed in Table 4.

4 DATA REDUCTION

Reduction of circular polarisation data is fully explained in Bagnulo & Landstreet (2018) and references therein. Most of the steps used to reduce linear spectropolarimetric data are

similar to the procedure for reducing circular polarisation data, but additional steps have to be taken to correct linear polarisation measurements for the chromatism of the retarder waveplate. Also, because sky background may be linearly polarised, its subtraction is particularly crucial. These steps will be described in Sect. 4.1 and 4.2 below.

4.1 Correction for the chromatism of the retarder waveplate

The position angle of the optical axes of the retarder waveplate is wavelength dependent, therefore the measured position angle will be affected by a (wavelength-dependent) offset $\epsilon(\lambda)$, which may be estimated by measuring the polarisation angle of a source for which the polarisation position angle is well known. Following Bagnulo et al. (2009), the reduced Stokes parameters were obtained from the observed P'_Q and P'_U using

$$\begin{aligned} P_Q(\lambda) &= P'_Q(\lambda) \cos(2\epsilon(\lambda)) + P'_U(\lambda) \sin(2\epsilon(\lambda)) \\ P_U(\lambda) &= -P'_Q(\lambda) \sin(2\epsilon(\lambda)) + P'_U(\lambda) \cos(2\epsilon(\lambda)) \end{aligned} \quad (2)$$

To calculate $\epsilon(\lambda)$ we have used observations of asteroid (2) Pallas that was observed by one of us (SB) on 2014-05-12 with ISIS in spectropolarimetric mode.

4.2 Background subtraction

Our observations of Grw+70° 8247 were obtained close to Full Moon. For a $V = 13.5$ target, the background level is relatively small, but because it is highly polarised, it may introduce spurious effects if not correctly subtracted (especially in the case of linear polarisation measurements). In both our linear polarisation measurements of Grw+70° 8247, the background level was about 10% of the source level, both in the blue and in the red spectral range. During the 2015 observations, the background polarisation was $\sim 36\%$ in the blue and $\sim 22\%$ in the red. In the 2018 observations, the background polarisation was about 51% in the blue and 28% in the red (see Sect. 5.5.4).

In ISIS, the background sky may be measured in four $5''$ strips (two per beam) parallel to the strips illuminated by the target, each separated by $18''$ from the central beam which is centred on the target (see the bottom panels of Fig. 1 of Bagnulo & Landstreet 2018).

We have experimented with different algorithms for background subtraction among those that are offered by the IRAF procedure `apall`, finding that our final results for the polarisation of Grw+70° 8247 were always consistent with each other within photon noise error bars. We have also carried out a more critical experiment as follows: instead of extracting the background from both full side strips, we used only a small window of one of the strips (of course still considering both beams split by the Savart plate). The results of this experiment were fully consistent (within error bars) with those obtained by estimating the background flux using both full strips. We are therefore satisfied that the presence of a non-negligible polarised backgrounds does not affect our data, e.g., by introducing a systematic effect, apart from reducing their S/N .

In contrast, our linear polarisation measurements obtained during the rejected night 2018-09-21 could not be

background subtracted, and the measured values were totally inconsistent with those obtained on the next night, when background subtraction could be correctly performed.

For circular polarisation, sky subtraction is a less critical step because the sky is not circular polarised. The effect of not subtracting the background would be a dilution of the polarisation signal by a factor roughly equal to the ratio between the sky flux and the star flux.

4.3 From spectropolarimetry to broadband polarimetry

Most of literature polarimetric data were obtained in broadband filters. For comparison purposes, it may be useful to compute synthetic broadband values using the formula

$$P_X(F) = \frac{\int_0^\infty d\lambda P_X(\lambda) I_X(\lambda) T_F(\lambda)}{\int_0^\infty d\lambda I_X(\lambda) T_F(\lambda)} \quad (3)$$

where T_F is the transmission function of the F filter and I_X is the sum of the fluxes in all beams and all images used to obtain the reduced Stokes X parameter. The setting in the blue ISIS arm that we have used for the observations of the magnetic white dwarfs covers the B filter, and the setting in the red ISIS covers the spectral range of the R filter. After integrating the signal over a large wavelength interval, photon noise error becomes totally negligible, but systematics and other effects are still present. As tentative estimates of the uncertainties of the broadband polarisation (BBP) values we will adopt the values obtained by replacing P_X in Eq. (3) with the corresponding null profiles N_X , with the caveat that this method still leads to an underestimate of the errors, as it would not include, for instance, telescope and instrumental polarisation, or errors in matching the original filter transmission function or detector wavelength sensitivity function.

5 QUALITY CHECKS

In the following we investigate the instrument accuracy and stability. We examine various potential issues that may affect the accuracy of our measurements: cross-talk from I to V (Sect. 5.1), from I to Q and U (Sect. 5.2), and from Q and U to V (Sect. 5.3). We present observations of magnetic stars and standard stars for linear polarisation that we have performed to check the correct alignment of the polarimetric optics (Sect. 5.4 for circular polarisation measurements and Sect. 5.5 for linear polarisation measurements). In Sect. 5.6 we discuss whether the use of a dichroic introduces a signal of spurious polarisation, as warned by the ISIS user manual. In Sect. 5.7 we discuss the polarimetric efficiency at shorter wavelengths. All results are then summarised in Sect. 5.8.

5.1 Estimate of instrumental circular polarisation in the continuum

The large majority of nearby WDs have a spectrum that is intrinsically unpolarised. Our extensive surveys of WDs (see [Bagnulo & Landstreet 2018](#)) offer abundant material to determine whether the instruments that we have used introduce a spurious signal of circular polarisation. For ISIS, we

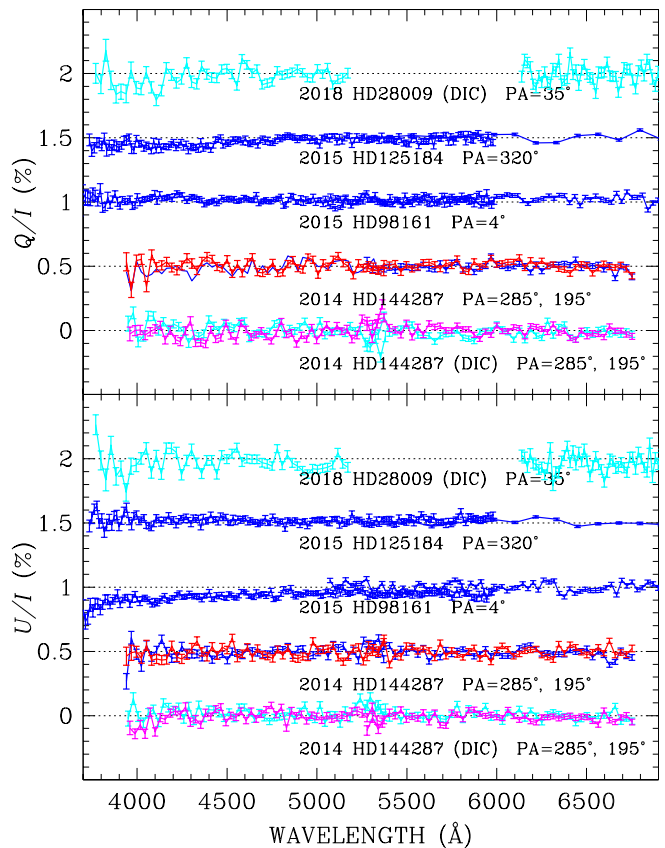


Figure 1. Polarisation spectra of unpolarised stars, offset in 0.5% steps for display purpose. Observations labeled with “DIC” (represented with light blue and magenta colour) were obtained in both arms simultaneously using a dichroic beam splitter. The remaining observations (red and blue solid lines) were obtained independently in the two instrument arms. The spectra of HD 144287 were obtained with the instrument position angle at 195° (magenta and red lines) and 285° (blue and light blue lines).

have found that the signal of circular polarisation in the continuum is generally $\lesssim 0.03\%$ in the blue arm and $\lesssim 0.05\%$ in the red arm.

5.2 Observations of unpolarised stars in linear polarisation

During the course of various observing runs with ISIS in spectropolarimetric mode we have obtained a number of measurements in linear spectropolarimetric mode of unpolarised stars listed in Table 1 (in our list we have included star HD 98099 that being within 50 pc was deemed as probably non significantly polarised, although was never adopted as unpolarised standard star). Some observations have been obtained independently both in the red and in the blue arm (one after the other), and some have been obtained simultaneously in both arms with the use of a dichroic beam splitter. We note that using the highly-sensitive PlanetPol instrument, [Hough et al. \(2006\)](#) estimated that the spurious polarisation introduced by the telescope optical surfaces of the WHT is of the order of $1.5 \cdot 10^{-5}$. Assuming that this was

Table 1. Observations of zero polarised stars.

STAR	DATE yyyy-mm-dd	UT hh:mm	EXP (s)	PA (°)	setting	P_Q (%)	P_U (%)	P_Q (%)	P_U (%)	Ref.
						B	R			
HD 144287	2014-03-07	05:00	100	285	R600R	–	–	0.01±0.01	0.00±0.00	1
	2014-03-07	05:05	100	285	R600B	0.00±0.02	–0.01±0.02	–	–	
	2014-03-07	05:09	100	285	R600B+R600R	–0.02±0.03	0.02±0.03	–0.02±0.00	0.00±0.00	
	2014-03-07	05:28	120	195	R600R	–	–	–0.00±0.00	–0.01±0.00	
	2014-03-07	05:33	120	195	R600B	–0.03±0.00	–0.02±0.00	–	–	
	2014-03-07	05:38	120	195	R600B+R600R	–0.03±0.02	–0.01±0.02	–0.01±0.02	–0.01±0.02	
HD 98161	2015-01-06	05:33	240	4	R300B	0.02±0.09	–0.08±0.09	–	–	2
	2015-01-06	05:50	120	4	R158R	–	–	0.02±0.01	0.00±0.01	
HD 125184	2015-01-06	06:21	40	321	R158R	–	–	0.01±0.02	–0.01±0.01	1
	2015-01-06	06:24	40	321	R300B	–0.05±0.01	0.02±0.01	–	–	
HD 28099	2018-09-24	06:16	35	240	R600B+1200R	–0.03±0.00	–0.02±0.00	–0.01±0.00	–0.04±0.00	3

Key to references: **1.** [Serkowski \(1974\)](#) **2.** [Turnshek et al. \(1990\)](#) **3.** Not previously used as unpolarised reference star – see text.

still true during our observing run, any measured signal of spurious polarisation would come from the ISIS instrument.

[Hough et al. \(2006\)](#) argued that spurious linear polarisation introduced by the instrument could be characterised with the help of observations obtained with the instrument set at different position angles on sky. For instance, denoting with $P_Q^{(\alpha)}$, $P_U^{(\alpha)}$ the reduced Stokes parameters measured with the instrument position at PA = α on sky, one should measure:

$$\begin{aligned}
 P_Q^{(0)} &= q + P_Q^{\text{instr}} \\
 P_Q^{(90)} &= -q + P_Q^{\text{instr}} \\
 P_U^{(0)} &= u + P_U^{\text{instr}} \\
 P_U^{(90)} &= -u + P_U^{\text{instr}}
 \end{aligned} \tag{4}$$

where q and u are the reduced Stokes parameters intrinsic to the source. In general, for an arbitrary PA = α_0 ,

$$\begin{aligned}
 P_Q^{\text{instr}} &= \frac{1}{2} \left(P_Q^{(\alpha_0)} + P_Q^{(\alpha_0+90)} \right) \\
 P_U^{\text{instr}} &= \frac{1}{2} \left(P_U^{(\alpha_0)} + P_U^{(\alpha_0+90)} \right).
 \end{aligned} \tag{5}$$

Our measurements are summarised in Table 1 and in Fig. 1, and show clearly that instrumental polarisation seems consistently well within 0.1% in both Stokes parameters Q and U , with the exception of one observations of HD 98161. Star HD 144287 was observed twice with the instrument position angle rotated by 90°. Instrumental polarisation measured via Eq. (5) was found $\lesssim 0.05\%$ at all wavelengths.

Star HD 144287 was observed first with the dichroic, then independently without dichroic in the two arms. A comparison between the results shown no evidence that the use of dichroic leads to a spurious signal of linear polarisation in stars that are intrinsically unpolarised. We will come back to this point in Sect. 5.6.

5.3 Crosstalk from linear to circular polarisation

The optics that precede the retarder waveplate may transform linear into circular polarisation or viceversa. Observa-

tions of circular polarisation of a source that is strongly linearly polarised may be affected by cross-talk from linear to circular polarisation and may give a non null measurement even if the source is not intrinsically circularly polarised. This is a well known instrumental effect present for instance in the FORS instrument of the ESO VLT, in which it is believed that the instrument collimator (located *above* the polarimetric optics) transforms a few per cent of the linear polarisation into circular polarisation (see Sect. 7.4 of [Bagnulo et al. 2009](#)). To check whether ISIS at the WHT (which has no dichroic optics above the wave plates) suffers from this problem, we have observed HD 25443, a standard star for linear polarisation, in linear and in circular polarisation, both in the red and in the blue arm simultaneously, with the dichroic. We measured $\sim 5\%$ of linear polarisation (consistently with previous literature), 0.02% of circular polarisation in the blue and less than 0.05% in the red. Hence cross-talk from linear to circular polarisation is smaller than 1%. Because the typical linear polarisation of strongly magnetic white dwarfs is only a few percent, this crosstalk is an unimportant contributor to the error budget of V/I measurements.

5.4 Alignment of the optics for circular polarisation: observations of magnetic stars

The correct alignment of the polarimetric optics used to measure circular polarisation was checked by measuring stars with known magnetic fields. For the ISIS observations obtained in our 2015 run, this check is described by [Bagnulo & Landstreet \(2018\)](#). In our September 2018 run (on 2018-09-21 at 20:11 UT) we observed the magnetic Ap star γ Equ (= HD 201610) and measured a mean longitudinal field of -970 ± 30 G in the blue arm and -974 ± 26 G in the red arm. These values are perfectly internally consistent, and are consistent with what is expected for that long period ($P \gtrsim 100$ y) magnetic variable (see Sect. 5.1.3 and Table A.1 of [Bagnulo & Landstreet 2018](#)).

Table 2. Observations of standard stars for linear polarisation. Position angle is measured counterclockwise looking at the source from the great circle passing through the star and the North Celestial Pole. For comparison, literature data are reported in boldface fonts. Uncertainties are due to photon-noise, and do not take into account systematics. Observations marked with asterisks are likely to be affected by the contamination of a strong background for the reasons explained in the notes.

STAR	DATE	UT	EXP		P_L (%)	Θ ($^\circ$) <i>B</i>	$\Delta\Theta$ ($^\circ$)	P_L (%)	Θ ($^\circ$) <i>R</i>	$\Delta\Theta$ ($^\circ$)	
	yyyy-mm-dd	hh:mm	(s)	setting							
HD 161056	Schmidt et al. (1992)				3.80±0.60	66.6±0.4		4.01±0.03	67.3±0.2		
	2014-03-06	06:00	160	R600R				3.99±0.01	68.0±0.1	+0.7	
	2014-03-06	06:06	80	R600B	3.65±0.01	68.0±0.1	+1.4				
	2014-03-06	06:10	80	R600B+R600R	3.65±0.03	67.9±0.3	+1.2	4.00±0.01	68.1±0.1	+0.8	
HD 204827	Schmidt et al. (1992)				5.65±0.02	58.2±0.1		4.89±0.03	59.1±0.2		
	2015-01-05	19:24	80	R158R				4.93±0.02	59.7±0.1	+0.6	
	2015-01-05	19:32	240	R300B	5.73±0.00	58.6±0.1	+0.4				
HD 154445	Schmidt et al. (1992)				3.45±0.05	88.9±0.4		3.68±0.07	88.9±0.6		
	2015-02-04	06:35	160	600B	3.44±0.04	89.5±0.3	+0.6				
HD 160529	Hsu & Breger (1982)				6.97±0.03	20.1±0.1		7.04±0.01	20.8±0.1		
	2015-08-30	20:28	80	R1200R				6.97±0.00	19.7±0.0	-1.1	
	2015-08-30	20:35	240	R600B	6.97±0.02	19.1±0.1	-1.0				
	2015-08-30	20:42	120	R600B+R1200R	6.94±0.00	19.2±0.0	-0.9	6.93±0.00	19.7±0.0	-1.1	
	2015-08-30	20:48	240	R1200R				6.97±0.00	19.4±0.1	-1.4	
HD 25443	Schmidt et al. (1992)				5.23±0.09	134.3±0.5		4.73±0.05	133.7±0.3		
	2014-03-11	20:31	480	300B	5.12±0.02	135.9±0.1	+1.6				
	2014-03-11	21:03	80	158R				4.80±0.01	135.3±0.0	+1.6	
	2015-01-06	00:17	80	R158R				4.76±0.04	135.4±0.2	+1.7	
	2015-01-06	00:24	320	R300B	5.11±0.02	135.7±1.4					
	(*)	2015-08-31	06:28	120	R1200R				4.91±0.00	136.6±0.0	+2.9
	(*)	2015-08-31	06:34	120	R600B	5.16±0.02	136.0±0.1	+1.7			
	(*)	2015-08-31	06:38	100	R600B+1200R	5.03±0.00	135.1±0.0	+0.8	5.11±0.00	135.5±0.0	+1.8
	(**)	2018-09-22	03:57	480	R600B+1200R	5.11±0.01	138.1±0.1	+3.8	4.87±0.02	137.9±0.1	+3.2
	HD 19820	Schmidt et al. (1992)				4.70±0.04	115.7±0.2		4.53±0.03	114.5±0.2	
(**)	2018-09-22	03:42	480	R600B+R1200R	4.59±0.02	118.4±0.1	+2.7	4.55±0.02	117.0±0.1	+2.5	
BD+59 389	Schmidt et al. (1992)				6.35±0.04	98.1±0.2		6.43±0.02	98.1±0.1		
(**)	2018-09-22	03:25	720	R600B+R1200R	6.20±0.03	102.0±0.2	+3.9	6.48±0.02	101.1±0.1	+2.0	

(*) Observations were obtained close to sunrise; sky background was high and rapidly increasing from one exposure to the next.

(**) Observations were taken with a wrong combination of dekker and window readout, therefore sky background could not be measured and subtracted.

Table 3. Calibrations of the polarisation position angle in the blue arm

OBJECT	DATE	UT	Θ ($^\circ$)		$\Delta\Theta$ ($^\circ$)
	yyyy-mm-dd	hh:mm	Expected	Observed	
Moon	2015-02-01	20:16	175.8	175.7±1.1	-0.1
	2015-09-01	06:06	159.0	159.0±0.4	0.0
	2018-09-22	19:38	151.8	151.7±0.2	-0.1
Twilight	2018-09-22	19:38	3.8	5.1±0.0	+1.3
	2018-09-23	19:09	0.6	179.7±0.1	-0.9
Background	2015-09-01	00:17	3.9	1.7±0.3	-2.2
	2015-09-22	21:01	39.2	39.6±0.3	+0.4

5.5 Alignment of the optics for linear polarisation

Since we aim to detect subtle variations of the polarimetric properties of the target star, we need to pay special attention the correct alignment of the polarimetric optics. This was checked with the help of measurements of standard stars for linear polarisation (Sect. 5.5.1), of the Moon (Sect. 5.5.2),

of the twilight sky (Sect. 5.5.3) and of the background sky during our science observations (Sect. 5.5.4).

5.5.1 Observations of standard stars for linear polarisation

The most obvious check to do is to observe standard stars for linear polarisation and compare the results with literature data. In order to assess the overall instrument stability we have considered ISIS data obtained in a period of time more extended than the epochs of the science observations presented in this paper. Since literature data report measurements in broadband filters, we have used Eq. (3) to integrate the spectra obtained in the blue arm with the *B* filter response curve, and the spectra in the red arm with the *R* filter response curve. In Table 2 we report all our observations of standard stars, even those that we suspect are affected by spurious signals. Our objective is not to establish a list of standard stars but to characterise the instrument and in particular check its stability. Results that are slightly

off from expectations are still useful to help to evaluate what can go wrong during spectropolarimetric observations.

It appears that, apart from the cases flagged in the Table footnotes, the position angle of the polarisation of standard stars is always within 1° of the literature data, and polarisation values differed at most by 0.1%. In the context of this investigation, these discrepancies are not significant, our conclusion is that ISIS observations of standard stars for linear polarisation confirm that the instrumental systematics are at most 0.1-0.2% and $1 - 2^\circ$. When not dominated by photon noise, uncertainties should be generally of that order of magnitude.

5.5.2 The position angle of the polarisation of the Moon

The light scattered by the atmosphere-less objects of the solar system is polarised in the direction either parallel or perpendicular to the scattering plane. The angle Φ between the scattering plane and the great circle passing through the region of the sky pointed by the telescope and the North Celestial Pole can be obtained from the relationship (Bagnulo et al. 2006)

$$\frac{\sin \delta_{\text{Tel}} \cos(\alpha_0 - \alpha_{\text{Tel}})}{\cos(\delta_{\text{Tel}}) \tan(\delta_0) - \sin(\alpha_0 - \alpha_{\text{Tel}}) \frac{1}{\tan(\Phi)}}, \quad (6)$$

where (α_0, δ_0) represent the coordinates of the Sun and $(\alpha_{\text{Tel}}, \delta_{\text{Tel}})$ the coordinates of the observed target, in this case the Moon.

The Moon was observed at the beginning of each night of our observations. On 2015-09-01 and 2018-11-22, the Moon phase-angle (the angle between the Sun, the Moon and the observer, not to be confused with the angle Φ which identifies the position of the scattering plane in the plane of the sky) was 25° and 20° . At these phase-angles, the (small) lunar polarisation is expected to be perpendicular to the scattering plane, and our measurements were found within $1-2^\circ$ of the expected value $\Phi + 90^\circ$.

5.5.3 Position angle of the polarisation of the twilight sky

Assuming a single scattering mechanism, the light scattered by the sky should be polarised in the direction perpendicular to the scattering plane. We verified that the position angle of the polarisation of the twilight sky was consistent with the value of $\Phi + 90^\circ$, where Φ is again obtained from Eq. (6), in which (α_0, δ_0) are the coordinates of the Sun and $(\alpha_{\text{Tel}}, \delta_{\text{Tel}})$ are the coordinates of the point on the sky pointed by the telescope.

5.5.4 Position angle of the polarisation of the background sky

The polarisation of the background sky of science observations may be accurately measured if exposures are sufficiently long and/or background intensity is sufficiently high, for instance because of the presence of the Moon. One can compare the direction of the polarisation of the background sky and verify that it is perpendicular to the scattering plane. During our science exposures, the background was illuminated (and highly polarised) because of the presence of a nearly full Moon (see Sect. 4.2). We found that the

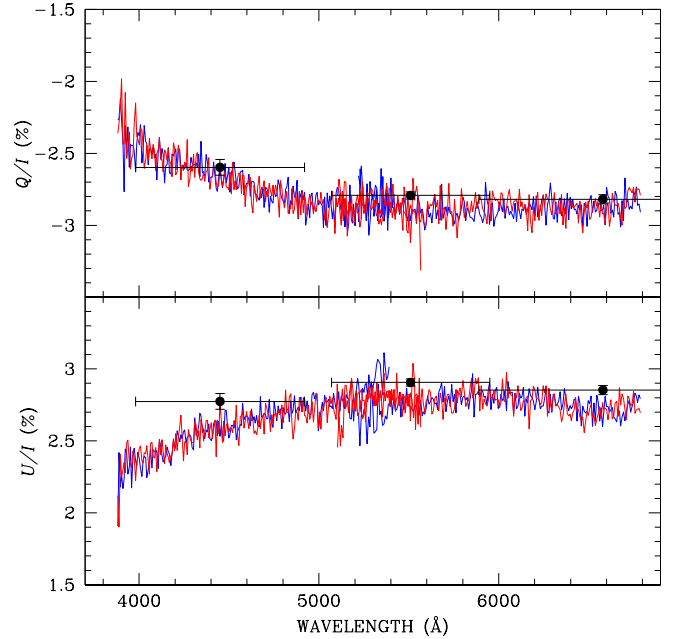


Figure 2. Polarisation spectra of star HD 161056 obtained on 6 march 2014 using the dichroic (blue lines) and observing in the two arms separately, without the dichroic (red lines). Solid circles represent the broadband linear polarisation values from Schmidt et al. (1992) (horizontal errorbars corresponds to the filter FWHM).

direction of the background sky was oriented within a few degree of the value $\Phi + 90^\circ$ as obtained from Eq. (6), where (α_0, δ_0) are the coordinates of the Moon and $(\alpha_{\text{Tel}}, \delta_{\text{Tel}})$ the coordinates of Grw+70° 8247.

5.6 Does the dichroic produce a spurious polarisation signal?

The ISIS spectrographs has two different camera arms, one optimised for the red and one for the blue. The insertion of a dichroic beam splitter allows one to observe simultaneously with both arms. This is a very valuable instrument feature that doubles the diagnostic capabilities compared to a situation in which the two arms are fed individually in separate exposures. The instrument web pages suggests that light scattered by the back of the dichroic may compromise polarimetric measurements, and that therefore observations in spectropolarimetric mode should not be carried out in both arms simultaneously. In Sect. 4.2.2 of Bagnulo & Landstreet (2018) we found that magnetic field measurements obtained with the dichroic inserted in the optical path do not differ significantly from those obtained when the blue and red arm are fed separately. Table 2 shows that our observations of linear polarisation obtained with the dichroic are consistent with literature data, suggesting that spurious effects introduced by the dichroic, if present at all, are probably not very significant. Moreover, in 2015, the standard star for linear polarisation HD 160529 was observed with the dichroic in the blue and red arms, and also (quasi-simultaneously) in the blue and red arm individually (see Fig. 2 and Table 2). A similar observation was carried out

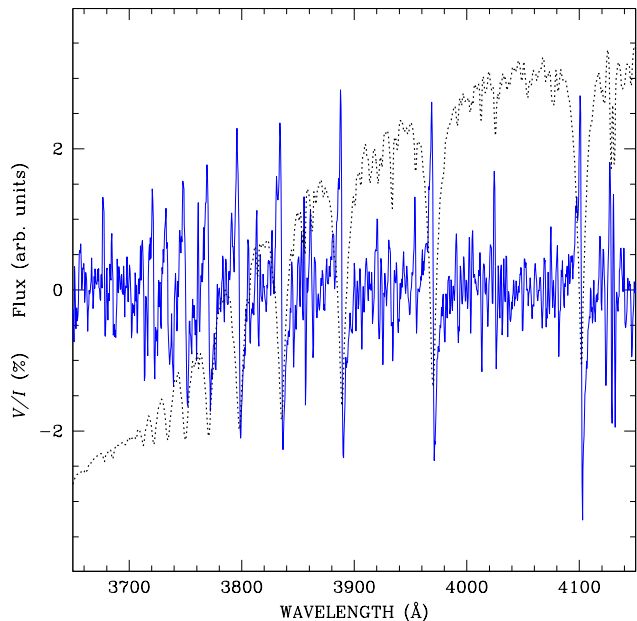


Figure 3. The polarised spectrum of the magnetic Ap star HD 215441 shows that the optical properties of ISIS are stable at shorter wavelengths.

on 6 March 2014 on the standard star HD 160556 and on the unpolarised star HD 144287 (see Table 1). The results of these two experiments do not point to spurious effects introduced by the dichroic. Therefore, even if the possibility that scattered light may affect polarimetric measurements should not be forgotten, we proceed assuming that the measurements obtained with the dichroic are not affected by significant spurious effects.

5.7 Polarimetric behaviour at shorter wavelengths

In Sect. 8 we will see that at $\lambda \lesssim 4000 \text{ \AA}$, the ISIS circular polarisation spectrum of Grw+70° 8247 shows remarkable differences compared to previous data obtained in the 1970s. To explore whether the observed changes are due to an instrumental effect (for instance a dramatic change of the retardation or the position angle of the fast axis of ISIS retarder waveplate), we have inspected the polarisation spectrum of the strongly magnetic Ap star HD 215441 that we obtained in 2015 (Bagnulo & Landstreet 2018) with the same setting as Grw+70° 8247 (see Fig. 3). Visual inspection shows that the higher order Balmer lines appear polarised in a similar way as H γ and H β (taking into account the fact that Zeeman effect varies as λ^2). In a more quantitative way, the longitudinal magnetic field calculated from each individual Balmer line via Eq. (1) gives the same result (within error bars). We conclude that, in the observed spectral range, the chromatism of the quarter retarder waveplate is not responsible for obvious artefacts.

5.8 Summary

To summarise the results of this Section:

- We find negligible zero point polarisation present in observations of both circular and linear polarisation made with ISIS in spectropolarimetric mode.
- We find negligible crosstalk between Stokes components Q , U , and V in ISIS data.
- Both the scale and position angle deduced from ISIS linear spectropolarimetry are extremely accurate.
- Our methods for correcting for polarised night sky contaminating spectra of faint objects are robust and reliable.
- We did not find any evidence that the use of a dichroic beam-splitter with cut-off at 5300 \AA produces a signal of spurious polarisation.
- We did not find evidence for artefacts due to the chromatism of the quarter waveplate.

6 OBSERVATIONS OF GRW+70° 8247

In the late 1960s James Kemp, an experimental physicist at the University of Oregon, realised that thermal emission from an incandescent body in a very strong magnetic field should display broad-band (spectrally diffuse) circular polarisation, at a level of the order of $10^{-2} \%$ for a field of 10^5 G (Kemp 1970). He showed experimentally that this idea is qualitatively correct (Kemp et al. 1970a). When he heard from George Preston of the Hale Observatories that efforts were being made to detect large fields in white dwarf stars (Preston 1970; Angel & Landstreet 1970a), he adapted his laboratory polarimeter for astronomical observations and started a search for circular polarisation due to magnetic fields in bright WDs on the 24-inch telescope of the University of Oregon’s Pine Mountain Observatory.

At the suggestion of one of us (JDL), Kemp observed Grw+70° 8247 and promptly detected strong circular polarisation. Following a telephone call from Kemp, three confirming measurements were obtained by Angel and Landstreet at Kitt Peak National Observatory, using the photoelectric polarimeter described by Angel & Landstreet (1970a). These measurements showed circular polarisation increasing with wavelength from about 1.5% at 380 nm to 3.3% at 620 nm. These observations represented the first discovery of a magnetic field in a white dwarf (Kemp et al. 1970b).

This result triggered a number of further surveys for magnetic fields in WDs, which up to the present have led to the identification of several hundred MWDs (Ferrario et al. 2015). Grw+70° 8247 still has one of the strongest WD magnetic fields known. It is often considered to be a star with a constant signal of circular polarisation. However, it has not been monitored nearly as frequently as one could have imagined. In the following we will review the polarimetric measurements that are found in the literature (Sect. 6.1 and 6.2), before presenting our new data (Sect. 6.3) and comparing them with earlier datasets (Sect. 8).

6.1 Observations of circular polarisation in the literature

In this and in the following Sections we will report the sign of circular polarisation using our definition of Sect. 2. Therefore, some numerical values may appear with the opposite sign with respect to that found in the original papers.

After the discovery by Kemp et al. (1970b), Angel &

Landstreet (1970b) reported a number of measurements of circular polarisation of Grw+70° 8247 obtained between 20 June and July 7 1970, made using the photoelectric polarimeter described by Angel & Landstreet (1970a). No on-sky calibration sources were known for circular polarimetry, and the instrument performance was tested using circular polarisers. Observations were obtained without any filter, covering the spectral range 400 to 700 nm (see Table 1 and Fig. 1 of Angel & Landstreet 1970b). The circular polarisation was found to be constant with time over an interval of days.

Circular polarisation was also measured in eight different wavelength windows from 310 to 800 nm, using filters with estimated FWHM between 30 and 120 nm (see Table 2 and Fig. 2 of Angel & Landstreet 1970b). These data provided a very low resolution ($R \sim 10$) spectrum of the wavelength dependence of the circular polarisation of Grw+70° 8247. The peak circular polarisation was about 3.7%, around 415 nm.

Kemp & Swedlund (1970) measured circular polarisation in the infrared, but we will not follow up further on this spectral region.

Angel et al. (1972) reported further polarimetric monitoring of the star, which was observed again during four observing runs in late 1970 and early 1971 in circular polarisation, using a variety of filters. These measurements are compared with the earlier filter polarisation data. They appear to rule out substantial changes on a time scale of months shortward of 600 nm. Angel et al. (1972) noted a possibly real variation of circular polarisation at $\lambda = 740$ nm, where circular polarisation decreased from about 2.4% in 1970 to about 1.0% in 1972, but this could have been due to the different red sensitivity of two different photomultipliers, one with S-20 red response and one with GaAs photocathodes, used in the polarimeter during this period.

The spectrum of circular polarisation was measured in June 1971 with higher spectral resolution (resolution 80 Å below about 5500 Å, and 160 Å above, or resolving power $R \sim 40 - 50$), using the multichannel spectrophotometer (MCSP) on the 200-inch Hale telescope on Mount Palomar, which was converted into a spectropolarimeter with the addition of a Pockels cell waveplate followed by a polariser in front of the entrance aperture (Angel et al. 1972). Globally this polarisation spectrum is in agreement with the very low-resolution spectrum found with filters, but it has high enough R to begin to reveal spectral features in Stokes V/I associated with weak absorption features in the Stokes I .

Landstreet & Angel (1975) reported further observations using the MCSP as a spectropolarimeter. The circular polarisation spectrum observed in August 1972 was compared to a new, very similar V/I spectrum from June 1973. Both were taken with spectral resolution of 80 Å in the blue and 160 Å in the red. No strongly significant differences among the three MCSP V/I spectra were detected, suggesting that any changes occur on a time of a decade or more.

One more circular polarisation spectrum was taken in 1976 in the spectral window 4–7000 Å. This spectrum, which has strongly variable resolution decreasing towards the red, was obtained using a prism spectropolarimeter with a Digicon detector on the Steward Observatory 2.3-m telescope (Angel et al. 1985). This spectrum was digitised from the

published graph for this paper². Apart from a few differences due to the different resolving power of the Palomar and Steward spectra, all the circular polarisation spectra from the 1970s appear essentially identical. When the large differences in resolving power are taken into account, the polarised spectra are also in general agreement with the results of filter polarimetry. Overall, the available data show no convincing evidence for variability over the period of about six years during the 1970s when the star was actively observed.

Putney (1995) published a circularly polarised spectrum of Grw+70° 8247 (see her Fig. 3), with a 11.1 Å spectral resolution, in the spectral range 3900–8900 Å. The spectrum was presented as “unpublished data” from Keck, and used for comparison with the spectra of other MWDs. We assume that were obtained around the time of other similar spectra presented in the paper, i.e., late 1994 or early 1995. Also this spectrum was digitised by us for its use in this paper.

WHT archive data revealed that the star was observed a number of times with the ISIS instrument, both in spectroscopic and spectropolarimetric mode. In this paper we consider circular spectropolarimetric observations obtained in 2004-08-05 at UT 21:28, obtained for a total 480 s exposure time with grating R600B in the wavelength range 4000 – 5200 Å and a 1.12'' slit width. Setting is very similar to what we have used in the blue arm, except that, compared to our data, the archive spectrum is offset by about 450 Å to the red. A lower S/N ratio spectrum was obtained the next night and appears consistent with the one obtained on August 5, within photon-noise error bars.

Grw+70° 8247 has been used as a standard star for circular BBP by Butters et al. (2009), who report measurements in the $UBVRI$ filters consistent with previous literature (see their Table 5), e.g. 3.6, 4.0 and 4.1% in the B , V and R filters, respectively. We have found in the literature no other published monitoring of circular BBP of this star.

6.2 Observations of linear polarisation in the literature

In addition to a series of circular polarisation measurements (Sect. 6.1), Angel & Landstreet (1970b) discovered strong linear polarisation, and measured the relevant Stokes parameters using four different filters in the spectral range between 310 and 700 nm. They detected a peak polarisation around 380 nm of 3.7% (but no linear polarisation at $\lambda \gtrsim 500$ nm), with a position angle in the blue between 16° and 24°. Angel et al. (1972) reported similar values measured in September 1970 and July 1971.

A single MCSP linear polarisation spectrum, observed with resolutions 160 and 360 Å (in blue and red respectively) in August 1972, in the range 329 to 1092 nm, was reported by Landstreet & Angel (1975); they also reported a private communication from Gehrels suggesting detection of a rotation of the position angle at 560 nm.

Another MCSP linear polarisation spectrum, very similar to the one reported by Landstreet & Angel (1975) was obtained on 28 April 1975 by Angel and Landstreet (unpublished). Over most of the spectral window studied, these

² Using software available at <https://automeris.io/WebPlotDigitizer/>

two Palomar linear polarisation spectra are very similar but perhaps not quite identical.

A single linear polarisation spectrum, very similar to the circular polarisation spectrum from the Steward Observatory team described in the previous section, was obtained in 1976 by [Angel et al. \(1985\)](#). This spectrum (digitised as for the circular polarisation spectrum from the same paper) shows somewhat more significant changes relative to the two Palomar linear polarisation spectra. Some of these differences are certainly due to the markedly higher resolving power of the Steward spectrum relative to the Palomar spectra in the blue, but other differences, between 5500–6500 Å, may possibly be real. Overall, however, these data, together with the BBP observations, do not provide convincing evidence of variability of the linear polarisation during the 1970s.

[West \(1989\)](#) obtained a single BBP measurement during 1986 in the *B* filter: 3.19% with $\Theta = 19^\circ.76$.

[Friedrich & Jordan \(2001\)](#) searched for variability due to rapid rotation of linear polarisation using a trailing technique at the 2.2 m telescope of Calar Alto in the Johnson *B* filter. They confirmed that the linear polarisation of the star is not variable on a time-scale of minutes.

6.3 New intensity and polarisation spectra

Our new data consist of intermediate resolution flux and polarised spectra obtained in 2015 and 2017.

In the MWDs with the largest fields, the spectral features of the intensity spectrum are often shallow, and display low contrast with respect to the continuum, hence they might not be obvious to the eye. In an effort to make these features stand out more clearly without requiring extremely accurate flux calibration of our spectra, we have experimented the use of the quantity $\delta\mathcal{F}_N$. This is defined as the difference between the intensity spectrum as observed (\mathcal{F}) and its smoothed version \mathcal{F}_s , normalised to the smoothed spectrum:

$$\delta\mathcal{F}_N = \frac{\mathcal{F} - \mathcal{F}_s}{\mathcal{F}_s} \quad (7)$$

where the smoothed intensity spectrum is calculated with a Fourier filter N Å wide. Obviously, this quantity is prone to enhance not only stellar features but also spectral features due to the Earth's atmosphere and spurious instrumental effects (for example coming from the CCD). However, this function is found to be very helpful in identifying various spectral features in the intensity spectrum, therefore we have decided to adopt it.

Figure 4 presents both archival and new polarisation spectra of Grw+70° 8247. Table 4 gives the observing log and reports the broadband values of our new polarisation spectra calculated via Eq. (3).

From top to bottom, the various panels of Fig. 4 show 1) the measured (unpolarised) flux \mathcal{F} , not corrected for the instrument transmission function; 2) the difference $\delta\mathcal{F}_{300}$ defined by Eq. (7) (limited to our new WHT data only); 3) the reduced Stokes parameter V/I ; 4) the reduced Stokes parameter Q/I ; 5) the reduced Stokes parameter U/I ; 6) the fractional linear polarisation P_L ; and 7) the polarisation position angle Θ . Literature data shown in Fig. 4 are those obtained at Mount Palomar in 1972 (circular and linear),

1973 (circular only), and 1975 (linear only), as well as the Steward spectra (linear and circular) from 1976.

The interpretation of the spectrum of Grw+70° 8247 remained a mystery for more than a decade after the discovery of its magnetic field. The main spectral line features were identified when calculations of the wavelengths of line components of the spectrum of hydrogen in fields of hundreds of MG were successfully made by [Roesner et al. \(1984\)](#). Using these data, [Angel et al. \(1985\)](#) were able to account qualitatively for all the principal absorption features in the optical spectrum as being due to H in a magnetic field ranging in strength between about 160 and 320 MG. This interpretation of the observed Stokes *I* spectrum was confirmed by comparison calculations of [Jordan \(1992\)](#), who however showed that the atomic data were not yet sufficient to make possible modelling of the polarisation spectra.

In the blue ISIS spectrum, the well-known Minkowski band at 4135 Å ([Greenstein & Matthews 1957](#)) stands out spectacularly both in $\delta\mathcal{F}_N$ and in Stokes Q/I , U/I and V/I . Other Minkowski bands at 3650 Å and 4466 Å are also visible. Additional, somewhat weaker but apparently real absorption features confirmed by corresponding polarisation features are found at about 4300 Å, 4480 Å, and possibly at 4950 Å. Corresponding absorption lines are seen in some of the model Stokes *I* spectra computed by [Jordan \(1992\)](#); because these are quite weak features in the raw Stokes *I* spectrum, it is not clear if most of them are present in the observed *I* spectrum of [Angel et al. \(1985\)](#). A very weak feature in the Stokes *I* spectrum at 6650 Å also corresponds to weak but quite clear feature in the $\delta\mathcal{F}_N$, V/I and Q/I spectra. This feature may correspond to the $3s'0-2p+1$ component of $H\alpha$, which is stationary at about 6643 Å at a field strength of about 140 MG and appears in the syntheses of [Jordan \(1992\)](#).

7 BROADBAND POLARIMETRY MEASUREMENTS MAY NOT BE SUITABLE TO DETECT REAL VARIABILITY

Since this work is primarily devoted to the search for subtle variability of Grw+70° 8247 we make a preliminary comment about BBP measurements.

In the blue spectral region, the polarisation of Grw+70° 8247 changes rapidly with wavelength. Therefore, BBP measurements obtained with slightly different instrument settings may differ one from each other, even if the polarisation intrinsic to the star is constant. This can be easily seen via numerical simulations through Eq. (3), using the observed spectra but different filter transmission curves. As an example, Table 5 shows the integrated polarisation calculated using Eq. (3) and the transmission functions of three different broadband *B* filters: an old *B* Bessel filter used with the FORS instrument of the ESO VLT, the currently used FORS b_high filter, and the *B* Bessel filter used with the ACAM instrument of the WHT (filter transmission curves may be found in the respective instrument web pages). For Grw+70° 8247, the results differ by 0.2–0.3%, which may well be larger than uncertainties due to photon noise, and hence easily detected.

This exercise shows that subtle changes observed in

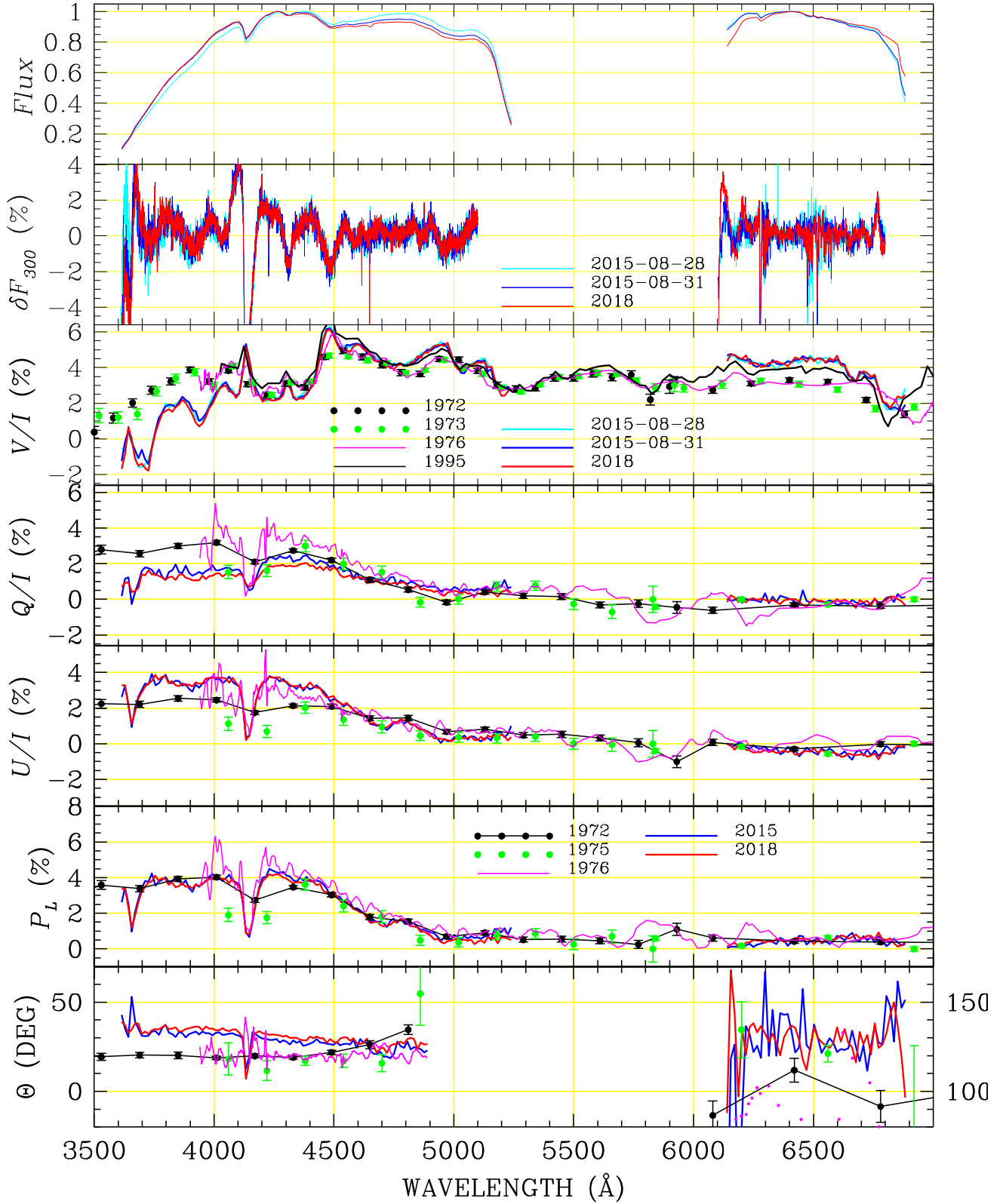


Figure 4. Polarisation spectra of Grw+70° 8247 obtained at various epochs. For display purposes, the position angle data Θ in the red ($\lambda \gtrsim 6000 \text{ \AA}$, see y axis on the right) are reported with a 100° offset with respect to the data in the blue ($\lambda \lesssim 5000 \text{ \AA}$, see y axis on the left). Keys to the symbols are given in the second panel from the top (for flux measurements) in the third panel from the top (for V/I measurements) and in the sixth panel from the top (for Q/I , U/I , P_L , Θ measurements). References are given in the text.

Table 4. Log of our new observations of Grw+70° 8247. We show also the BBP values obtained using the transmission curves of the old FORS B Bessel filter (cols. 3-7) and of the FORS Red Bessel filter (cols. 8-12). As in Table 2, uncertainties reflect photon-noise. Systematics errors are probably of the order of 0.1-0.2% at most for P_V , P_Q , P_U , and P_L , and $1-2^\circ$ for the position angle Θ . The large uncertainties of Θ in the red are due to the fact that linear polarisation is very small, hence its position angle not well determined. For the reasons explained in the text, these values are only internally self-consistent, and should not be compared to BBP measurements obtained with other instrument/telescopes.

DATE UT	EXP (s)	P_V (%)	P_Q (%)	B			Θ ($^\circ$)	P_V (%)	P_Q (%)	R		
				P_U (%)	P_L (%)					P_U (%)	P_L (%)	Θ ($^\circ$)
2015-08-28 22:10	1920	3.39±0.01						3.99±0.00				
2015-08-31 00:00	2400	3.37±0.02						3.99±0.01				
2015-09-01 00:17	2400		1.67±0.08	2.70±0.08	3.17±0.08	29.1±0.7			-0.04±0.08	-0.33±0.08	0.34±0.08	131.3±6.6
2018-09-22 21:51	1800	3.22±0.01						4.00±0.04				
2018-09-22 21:01	3600		1.40±0.04	2.74±0.04	3.08±0.04	31.5±0.4			-0.10±0.14	-0.43±0.14	0.44±0.14	128.6±9.0

Table 5. Polarisation of standard star HD 25443 and of MWD Grw+70° 8247 (observed on 2018-09-22) integrated in different B filters as explained in the text.

	HD 25443		Grw+70° 8247		
	P_L (%)	Θ ($^\circ$)	P_L (%)	Θ ($^\circ$)	P_V (%)
FORS B Bessel	5.11	138.1	3.08	31.5	3.22
FORS b_high	5.14	138.1	2.76	30.7	3.58
ACAM B Bessel	5.13	138.1	2.86	31.0	3.43

BBP measurements may actually be due to small differences of the transmission function of the instrument+telescope, rather than stellar variability. It is important to note that such differences due to different filters would not be detected in the observations of a standard star for linear polarisation. Table 5 shows that, due to its smooth behaviour with wavelength, the differences in the wavelength integrated polarisation of a standard star are of the order of 10^{-4} , i.e., some 10 times smaller than those calculated for Grw+70° 8247. Even using the same instrument and instrument setup for broad band measurement may not lead to conclusive results because instrument sensitivity may change over the years in a way not detectable through the monitoring of standard stars.

8 HAS THE POLARISED SPECTRUM OF Grw+70° 8247 CHANGED WITH TIME?

Inspection of the data from the 1970s in Fig. 4 confirms the conclusions of the original literature, i.e., that circular polarisation spectra obtained from 1972 to 1976 appear very similar to each other, and that the linear polarisation spectra obtained over the same period of time show at most some small differences in the blue spectral regions. Our new measurements obtained in 2015 and 2018 also seem *nearly* identical to each other.

Compared to the measurements in the 1970s, our new circular polarisation clearly show significant differences both in the red and at the shortest wavelengths. Linear polarisation shows obvious changes in the blue, and perhaps marginal differences in the red. Since about 40 years have

elapsed between the observations of Angel et al. (1972); Landstreet & Angel (1975); Angel et al. (1985) and our observations, polarisation measurements set a time scale for the changes of the order of decades or more.

In the following we inspect and comment on these differences in more detail.

8.1 Intensity spectra

ISIS data reveal that $\delta\mathcal{F}_N$ is constant within the 3-year interval of time from 2015 to 2018, both in the blue and in the red part of the observed spectrum. Unfortunately, we are not able to perform a meaningful comparison with intensity data obtained in previous decades.

8.2 Circular polarisation

As noted above, circular polarisation spectra obtained between 1972 and 1976 appear very similar to each other, as do the three circular polarisation spectra obtained by us in 2015 and 2018. However, when comparing datasets obtained 40 years apart, the amplitude of circular polarisation has changed significantly at $\lambda \lesssim 4000 \text{ \AA}$, between 4400 and 5000 \AA and between 6100 and 6700 \AA . Spectra obtained by Putney (1995) and WHT archive data obtained in 2004 show also some differences as discussed below.

8.2.1 The blue

The most remarkable variation in the circular polarisation spectra of Grw+70° 8247 is seen at $\lambda \lesssim 4000 \text{ \AA}$. Compared to the spectra obtained in the 1970s, circular polarisation is offset by about -1% . A careful inspection also shows that while the two datasets obtained in 2015 are fully consistent among themselves (within error bars), the polarisation measured in 2018 is slightly different precisely in those wavelength regions where large differences are detected when we compare data taken 40-45 years apart. This is best seen in Fig. 5. Differences between 2015 and 2018 datasets are tiny (e.g. $\sim -0.2\%$ at $\lambda \lesssim 4000 \text{ \AA}$). They are above the uncertainty due to photon noise, but not large enough to exclude that they are entirely due to some systematics. However, the fact that they appear in the same spectral region where large changes are seen in a 40-years interval of time suggests that

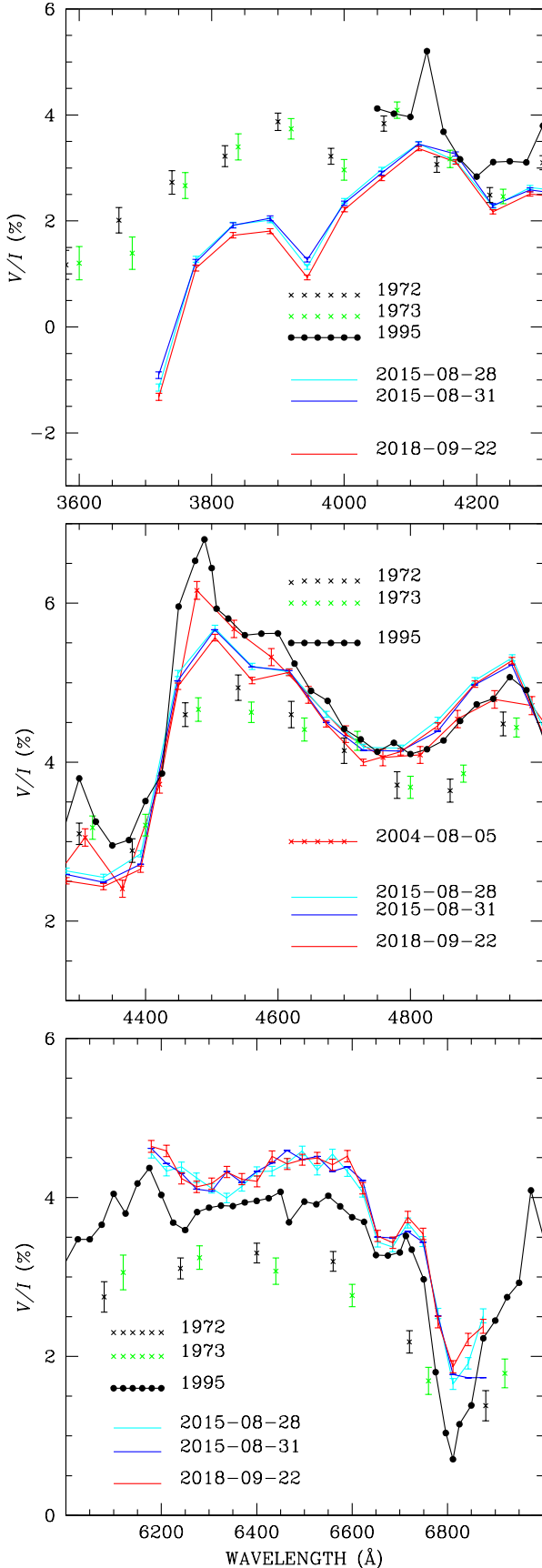


Figure 5. Enlarged view of circular spectropolarimetric data in spectral region covered by the ISIS instrument where discrepancies among datasets are noted.

the variability detected during a three-year span may well be intrinsic to the source (rather than due to an instrumental effect). Obviously this conclusion should be confirmed by further monitoring.

Differences are prominent also between 4400 and 4600 Å, where circular polarisation had a maximum in 1995, then decreased in 2004 and continued to decrease in 2015 and 2018.

Due to the large variations of the polarisation in the Minkowski bands, a comparison between our measurements synthetically integrated in the blue (3.43% in a *B* Bessel filter) and the $3.61 \pm 0.11\%$ value measured in the *B* filter by [Butters et al. \(2009\)](#) is not meaningful, apart from confirming that the polarisation does not change much within a time-scale of a few years.

8.2.2 The red

Circular polarisation around 6500 Å seems to have increase by about 1.5% from the 1970s (when it was about 3%) to $\sim 4.5\%$ at the time of our observations. In this spectral region we have not detected any change between 2015 and 2018, but data obtained in 1995 were in between the values measured in the two epochs. At 6800 Å, data obtained by [Putney \(1995\)](#) show the lowest values among all datasets ($\sim 1\%$).

Our BBP measurements in the red (4.0% integrated over a *R* filter) are consistent with the relatively recent BBP measurement of [Butters et al. \(2009\)](#), who had detected a signal of $4.06 \pm 0.16\%$. In conclusion, we have clearly detected a change of 1.5% over a 40+ years interval, but we have found no evidence of change over a time-scale of the order of three years.

8.3 Linear polarisation

No large changes of the fraction of linear polarisation are detected either on a short (3-year) or long (40 year) time-scale. However, over a 40–45 year interval of time, the position angle has definitely changed by more than 10° both in the blue and in the red. In the following we look at the various linear polarisation spectra and their differences in more detail.

On the long time scale sampled by the difference between the 1970s data and our recent ISIS spectra (40 years), there definitely are changes. In particular, below 4000 Å, the recent level of linear polarisation sampled by *Q/I* seems to have decreased, while that sampled by *U/I* is larger. This corresponds to a very significant rotation of the position angle of the linear polarisation away from the value of $\sim 20^\circ$ found in the 1970's to about 33° in recent times.

We note that the measurement by [West \(1989\)](#) obtained 1986 suggests also a decrease of linear polarisation compared to the 1970s (3.19% in the *B* filter, for a position angle of 19.1 ± 0.8) but as discussed in Sect. 4.3 these kinds of comparison should be made with caution.

It is notable that although the circular polarisation is quite different from zero throughout the visible spectrum, the non-zero linear polarisation is present essentially below 5500 Å, with possible low-level features suggested by the Steward spectrum, but largely absent from the lower resolution MCSP data. The position angle in the red as measured

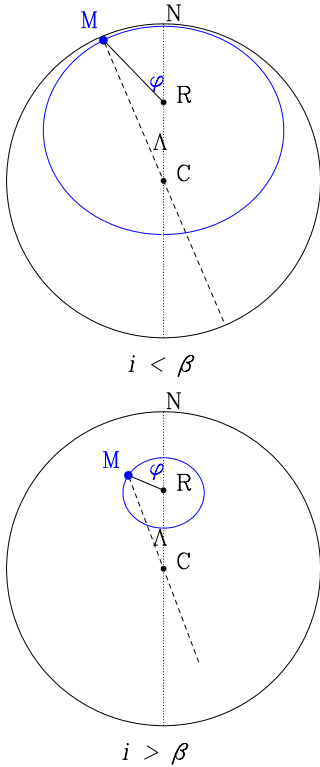


Figure 6. Two examples of oblique rotator model. The black solid lines represent the stellar disk; the centre of the stellar disc C , the rotation pole R and the North Celestial Pole N are aligned. M represents the magnetic pole at the surface of the star, and the blue solid line represents its trajectory on the stellar disk as the star rotates (φ represents the rotation angle). The dashed line represents the projection of the dipolar axis in the plane of the sky, and forms an angle Λ with the direction to the North Celestial Pole. *Left panel:* $\beta > i$ (as the star rotates, the position angle Λ spans monotonically the range 0 – 360° , and the polarisation position angle spans twice the range 0 – 180°). *Right panel:* $\beta < i$ (as the star rotates, the position angle Λ spans a limited angle range, and changes direction twice, and so does the polarisation position angle).

in the 1970s was around 110° , with a fair amount of scatter due to the small but not quite vanishing amplitude of Q and U in that region. In the ISIS data, both Q and U are also close to zero, therefore the position angle has a large uncertainty, but is consistent with a 10 – 30° rotation from the value measured in the 1970s.

We conclude that linear polarisation measurements are certainly variable over a time-scale of decades, mostly in terms of a rotation, while no significant variation has been detected on time scale of three years. A rotation constant in wavelength provides a first rough description of the change in linear polarisation.

9 CONSTRAINTS ON THE ROTATION PERIOD OF Grw+70° 8247

Measurements of the position angle of the broadband linear polarisation of Grw+70° 8247 in the blue between about 3800 and 4600 \AA may be used to try to detect evidence of

stellar rotation, under the assumption that the polarisation position angle Θ tracks the position angle of the magnetic axis Λ .

We assume that the star may be described by an oblique rotator model, with rotation axis tilted at an angle i with respect to the line of sight, and that the magnetic axis, for example a dipole axis, is tilted at an angle β with respect to the rotation axis. Formally, the angle i identifies the positive rotation pole, and the angle β identifies the positive magnetic pole, and both i and β may range from 0° to 180° (e.g. Landolfi et al. 1998). For simplicity, we will assume that $i \leq 90^\circ$ and $\beta \leq 90^\circ$, a situation to which one can always be brought back to, after reversing the rotation direction, the polarity of the magnetic field, or both (see Sect. 3 of Landolfi et al. 1998). None of these transformations will affect our conclusions below, which depend neither on the direction of the rotation, nor on the sign of the magnetic field.

There are two rather different geometrical situations that we should consider when interpreting time variations in the observed position angle of linear polarisation. One situation is when the tilt angle of the rotation axis i is smaller than the obliquity of the magnetic axis β , and one when the tilt angle i is larger than the obliquity β .

(1) When $i < \beta$, the position angle of the dipolar axis Λ will span the range 0 to 360° as the star rotates. This situation is visualised in the left panel of Fig. 6, and may be more easily understood by thinking of a star with the rotation axis parallel to the line of sight ($i = 0^\circ$) and the magnetic axis perpendicular to the rotation axis ($\beta = 90^\circ$). As the star rotates, the magnetic pole completes a 360° tour in the plane of the sky, and the polarisation spans twice the range 0 – 180° , always rotating in the same direction. Note, however, that the specific example of a rotation axis perpendicular to the line of sight implies that the longitudinal component of the magnetic field should be constant as the star rotates; this is not consistent with the observations of circular polarisation of Grw+70° 8247, which show variability with time.

(2) When $i > \beta$, the projected dipolar axis will not complete a full 360° as the star rotates, but would simply oscillate on the sky, changing direction every half rotation period (see the right panel of Fig. 6). The amplitude of the wobble of the position angle would be larger, the larger the value of β .

Because the position angle of linear polarisation may be quite precisely determined, searching for changes in the direction of the position angle is clearly a relatively straightforward method of detecting stellar rotation, unless the star rotates extremely slowly, or the field axis and the rotation axis are very closely parallel.

As we have detected rotation of the polarisation position angle, which we assume is due to rotation of the underlying star rather than significant evolution of the stellar magnetic field structure, it is of interest to try to obtain constraints on the stellar rotation period from the observations. Of course, we are severely limited by the obvious fact that we have not yet observed one full rotation, and so we do not yet know whether the geometry of the rotation axis and field obliquity is closer to case (1) or (2).

If the situation is close to case (1), with $i \leq \beta$, then a single rotation produces two full circles of the position angle on the sky. In this case we might have observed 10 – 15° of

a full 360° rotation in about 40 years, suggesting a rotation period of the order of one millenium.³

If Grw+70° 8247 is closer to case (2), the minimum possible period would correspond to our two main epochs of observation corresponding roughly to the two extremes of position angle oscillation. In this case another 40 or 50 years might bring the position angle back to about 20° . If this is the situation, the rotation period might be as short as a century.

In this discussion, we have made the implicit assumption that the polarisation position angle has monotonically changed during the last 40 years. In fact, we are not aware of linear polarisation measurements that can validate this. Also, we note that our period limit estimates are based on the assumption that $d\Lambda/dt$ is constant with time. This clearly cannot be true, around the epoch of inversion of the direction of changes of Λ , in scenario no. 2. Also, the effect of Faraday rotation may change as the star rotates, affecting also the assumption that $d\Lambda/dt$ is constant with time. However, our simple modelling should be sufficient for an order-of-magnitude estimate of the rotation period, which is all we can extract from the very limited available data. We conclude that the rotation period lies probably in the range of 10^2 to 10^3 yr.

Our period estimate may seem outrageously long, but there are main sequence stars known to have rotation periods near the lower limit, for example the star HD 201601 = γ Equ, with a period estimated to be about one century (Leroy et al. 1994; Bychkov et al. 2016). It is clear that physical processes exist that are capable of removing virtually all of a star's angular momentum, and that one of the most powerful of these processes acts through the stellar magnetic field.

10 CONCLUSIONS

We have presented new polarisation spectra of the white dwarf Grw+70° 8247, one of the most strongly magnetic of the known MWDs, and searched for variability.

To carry out our investigation, we had to perform a careful analysis of various polarimetric measurements obtained with the ISIS instruments in the last few years. We found some important results that help to characterise the instrument, and that may be useful to other users interested in the polarimetric capabilities at the WHT. In particular we found that:

- Both linear and circular instrumental polarisation are smaller (in absolute value) than 0.05 %.
- Cross-talk from linear to circular polarisation is negligible for most practical situations. Our estimate is that less than 1 % of the linear polarisation signal is transformed into circular polarisation.
- We found no evidence that the use of a dichroic beam

³ It was this argument, applied in the 1970s to an upper limit of perhaps 4° of position angle rotation in two years of observation, that led to the suggestion of a period of the order of 100 yr or longer (Landstreet & Angel 1975), which has frequently been repeated in the literature.

splitter introduces a spurious linear polarisation signal, confirming what was already found for circular polarisation by Bagnulo & Landstreet (2018).

- We have presented a list of ISIS observations of standard stars for linear polarisation to which we may refer in the future to monitor instrument stability,
- We have used lunar spectra, twilight spectra and background spectra to confirm the alignment of the polarimetric optics. This method may be adopted more systematically as it is probably faster and more accurate than observing standard stars.
- We have found inconsistencies between the way the circular polarisation of Grw+70° 8247 has been reported over the years; we have discussed the definition of the sign of circular polarisation, and clarified what we have adopted.

Regarding the scientific investigation of Grw+70° 8247:

- We have shown that spectropolarimetry in all four Stokes parameters (as opposed to broad band polarization measurement) is the method of choice for the study of strongly magnetic white dwarfs for two reasons. One is that only spectropolarimetry may reveal the shape of the Stokes profiles of the spectral features; the other is that it allows to discriminate between changes of the instrument sensitivity and changes of the polarisation intrinsic to the source.
- We have clearly established the variability of the polarisation spectra of the MWD Grw+70° 8247. We have argued that the observed rotation of the position angle of linear polarisation suggests that the rotation period is probably in the range of 10^2 to 10^3 yr. This result would imply that Grw+70° 8247 is one of the most slowly rotating stars known.

At this early stage in re-starting systematic observations of the highest-field MWDs, we hope that we have re-launched the systematic observation of these mysterious and potentially very important objects, which contain the largest fields in the universe that are easily observable directly in optical light. One of the long-term goals of this work is to obtain the observations needed to determine the rotation period of Grw+70° 8247, and to map the surface field structure, a task that we are obliged to leave to future generations of astronomers.

ACKNOWLEDGMENTS

This work is based on observations collected at the William Herschel Telescope, operated on the island of La Palma by the Isaac Newton Group, programmes P17 during semester 15B, and programme P15 during semester 18B. Important ISIS calibration data were obtained in the context of programme P5 during semester 14A, programme P30 during semester 14B, P28 during semester 15A. This paper has also made use of data obtained from the Isaac Newton Group Archive which is maintained as part of the CASU Astronomical Data Centre at the Institute of Astronomy, Cambridge. JDL acknowledges the financial support of the Natural Sciences and Engineering Research Council of Canada (NSERC), funding reference number 6377-2016. We thank Ian Skillen (ING) for calculating the instrument position angle on sky when the instrument and telescope were in the parking position, Tom Marsh for 2004 WHT data of

Grw+70° 8247 and Stefan Jordan for his useful review of this manuscript.

REFERENCES

- Angel J. R. P., Landstreet J. D., 1970a, *ApJ*, **160**, L147
- Angel J. R. P., Landstreet J. D., 1970b, *ApJ*, **162**, L61
- Angel J. R. P., Landstreet J. D., Oke J. B., 1972, *ApJ*, **171**, L11
- Angel J. R. P., Liebert J., Stockman H. S., 1985, *ApJ*, **292**, 260
- Babcock H. W., 1958, *ApJS*, **3**, 141
- Bagnulo S., Landstreet J. D., 2018, *A&A*, **618**, A113
- Bagnulo S., Szeifert T., Wade G. A., Landstreet J. D., Mathys G., 2002, *A&A*, **389**, 191
- Bagnulo S., Landstreet J. D., Mason E., Andretta V., Silaj J., Wade G. A., 2006, *A&A*, **450**, 777
- Bagnulo S., Landolfi M., Landstreet J. D., Landi Degl'Innocenti E., Fossati L., Sterzik M., 2009, *PASP*, **121**, 993
- Borra E. F., Landstreet J. D., 1980, *ApJS*, **42**, 421
- Butters O. W., Katajainen S., Norton A. J., Lehto H. J., Pirola V., 2009, *A&A*, **496**, 891
- Bychkov V. D., Bychkova L. V., Madej J., 2016, *MNRAS*, **455**, 2567
- Clarke D., 1974, in Gehrels T., ed., IAU Colloq. 23: Planets, Stars, and Nebulae: Studied with Photopolarimetry. p. 45
- Donati J.-F., Semel M., Carter B. D., Rees D. E., Collier Cameron A., 1997, *MNRAS*, **291**, 658
- Euchner F., Jordan S., Beuermann K., Gänsicke B. T., Hessman F. V., 2002, *A&A*, **390**, 633
- Euchner F., Jordan S., Beuermann K., Reinsch K., Gänsicke B. T., 2006, *A&A*, **451**, 671
- Ferrario L., de Martino D., Gänsicke B. T., 2015, *Space Sci. Rev.*, **191**, 111
- Friedrich S., Jordan S., 2001, *A&A*, **367**, 577
- Greenstein J. L., Matthews M. S., 1957, *ApJ*, **126**, 14
- Hough J. H., Lucas P. W., Bailey J. A., Tamura M., Hirst E., Harrison D., Bartholomew-Biggs M., 2006, *PASP*, **118**, 1302
- Hsu J.-C., Breger M., 1982, *ApJ*, **262**, 732
- Jordan S., 1992, *A&A*, **265**, 570
- Kemp J. C., 1970, *ApJ*, **162**, 169
- Kemp J. C., Swedlund J. B., 1970, *ApJ*, **162**, L67
- Kemp J. C., Swedlund J. B., Evans B. D., 1970a, *Physical Review Letters*, **24**, 1211
- Kemp J. C., Swedlund J. B., Landstreet J. D., Angel J. R. P., 1970b, *ApJ*, **161**, L77
- Kuiper G. P., 1935, *PASP*, **47**, 279
- Külebi B., Jordan S., Euchner F., Gänsicke B. T., Hirsch H., 2009, *A&A*, **506**, 1341
- Landi Degl'Innocenti E., Landolfi M., eds, 2004, Polarization in Spectral Lines Astrophysics and Space Science Library Vol. 307, doi:10.1007/978-1-4020-2415-3.
- Landi Degl'Innocenti E., Bagnulo S., Fossati L., 2007, in Sterken C., ed., Astronomical Society of the Pacific Conference Series Vol. 364, The Future of Photometric, Spectrophotometric and Polarimetric Standardization. p. 495 ([arXiv:astro-ph/0610262](https://arxiv.org/abs/0610262))
- Landolfi M., Landi Degl'Innocenti E., Landi Degl'Innocenti M., Leroy J. L., 1993, *A&A*, **272**, 285
- Landolfi M., Bagnulo S., Landi Degl'Innocenti M., 1998, *A&A*, **338**, 111
- Landstreet J. D., Angel J. R. P., 1974, *ApJ*, **190**, L25
- Landstreet J. D., Angel J. R. P., 1975, *ApJ*, **196**, 819
- Leroy J. L., Bagnulo S., Landolfi M., Landi Degl'Innocenti E., 1994, *A&A*, **284**, 174
- Mathys G., 2017, *A&A*, **601**, A14
- Preston G. W., 1970, *ApJ*, **160**, L143
- Putney A., 1995, *ApJ*, **451**, L67
- Roesner W., Wunner G., Herold H., Ruder H., 1984, *Journal of Physics B Atomic Molecular Physics*, **17**, 29
- Schmidt G. D., Elston R., Lupie O. L., 1992, *AJ*, **104**, 1563
- Schmidt G. D., Allen R. G., Smith P. S., Liebert J., 1996, *ApJ*, **463**, 320
- Serkowski K., 1974, in Gehrels T., ed., IAU Colloq. 23: Planets, Stars, and Nebulae: Studied with Photopolarimetry. p. 135
- Shurcliff W. A., 1962, Polarized light.
- Stibbs D. W. N., 1950, *MNRAS*, **110**, 395
- Turnshek D. A., Bohlin R. C., Williamson II R. L., Lupie O. L., Koornneef J., Morgan D. H., 1990, *AJ*, **99**, 1243
- West S. C., 1989, *ApJ*, **345**, 511
- Wunner G., Roesner W., Herold H., Ruder H., 1985, *A&A*, **149**, 102